

A COMPUTATIONAL STUDY OF THE GENERATION AND DECAY OF AIRCRAFT WINGTIP VORTICES

T.J. Craft, B.E. Launder, C.M.E. Robinson
School of Mechanical, Aerospace & Civil Engineering,
The University of Manchester,
Manchester M60 1QD, UK
tim.craft@manchester.ac.uk

ABSTRACT

Computations are reported of the flow over a NACA 0012 half-wing with rounded wing tip. The aim is to test the performance of a number of turbulence models in capturing the generation and near-field decay of the strongly accelerated vortex that is shed from the tip. Results using linear and non-linear eddy-viscosity models are presented, but these all exhibit too rapid a decay of the vortex core, and it is only an advanced stress transport model that is shown to reproduce many of the features found in the experimental measurements.

INTRODUCTION

The serious impact of the trailing vortices from large aircraft is well known. Many examples exist of the serious damage caused to following aircraft caught up in the swirling wake shed from an upstream aeroplane. While, at a practical level, guidelines exist for safe distances between aircraft, the issue of satisfactorily predicting the vortex formation and decay with CFD methods is far from being satisfactorily resolved. This is particularly relevant at the present time as there is considerable current research aimed at developing novel wing-tip devices to improve an aircraft's aerodynamic performance. Thus, attention needs to be given to examining the effect of such devices on the downstream decay of the trailing vortices and to exploring whether the devices may be explicitly designed to cause the vortices to decay more rapidly.

From a CFD standpoint, there are many challenges in correctly modelling the flow's development. The flow over the wing develops into a highly skewed three-dimensional boundary layer that, as it detaches, rolls up into a strong, nearly-axisymmetric trailing vortex. Swirling free flows are well known to be difficult to predict. Linear eddy viscosity models, unless empirically tuned for the specific flow under consideration, are virtually blind to the effects of streamline curvature that are so influential in this type of flow.

Our aim in the present work has thus been to examine the success of different turbulence models in capturing the flow's development. We have compared two locally-devised models (one the *non*-linear eddy-viscosity model of Craft et al. (1996), the other the two-component-limit (TCL) second-moment clo-

sure described in Craft & Launder (2001)) with two other models widely used in the aeronautics industry (Spalart & Allmaras, 1992; Kok & Spekreijse, 2000), and with the usual linear k - ϵ eddy viscosity model as a base reference. It is noted that since the TCL model correctly mimics the wall-vanishing of the pressure-strain term in the wall-normal component, there is no need to employ "wall-reflection" corrections of the type employed in earlier second-moment models.

The test case examined is the flow over a NACA 0012 half-wing with rounded wing tip examined by Chow et al. (1997). The airfoil is at a 10-degree angle of attack and, as advised by Professor Bradshaw, the experiments were conducted at a chord Reynolds number, Re_c , of 4.35×10^6 (rather than 4.6×10^6 as cited in Chow et al.). The wind tunnel had a width $1.0c$ and height $0.667c$, with the chord length $c = 48\text{in}$ (1.2192m). Transition was forced on both suction and pressure surfaces at 4% chord measured around the arc of the wing surface. A 7-hole pressure probe and hotwires provided mean and turbulence data. The most striking feature of their results was that at the centre of the shed vortex the axial velocity reached 1.77 times that of the approach velocity. Axial velocity peaks in shed vortices have been reported in several earlier studies though no group has previously reported a peak as high as 1.77. Although the whole wing has had to be computed, like the experiments, our attention in this paper is limited to the near-field development of the shed wing-tip vortex.

NUMERICAL & PHYSICAL MODELS

Turbulence Models

The main interest has been in seeing whether the complexities in the flow considered could be resolved with either of the models developed at UMIST specifically to overcome the inadequacies both of eddy-viscosity and conventional second-moment closures. The TCL model documented in Craft & Launder (2001) and Launder & Li (1994) has been in use for well over a decade and been found capable of handling a diversity of complex strain fields. For present purposes its two most important features are a model of mean-strain effects on the pressure-strain process fully consistent with the two-

component limit and a sink term in the dissipation rate (ε) equation dependent on the invariants of the Reynolds stress tensor; consequently it needs make no reference to distance of a point from a rigid boundary, an especial advantage in handling bodies of complex shape. A simpler route has also been tried, the non-linear eddy-viscosity scheme of Suga (see Craft et al., 1996). This was the first NLEVM to include cubic terms in the stress/deformation-rate constitutive equation, an elaboration essential to capture (approximately) the strong effects of streamline curvature on turbulence. The extra model coefficients thus introduced were fixed by considering a wide range of test flows including two wall flows with streamline curvature.

Two other models, widely used in the aerospace industry, were also examined: the Spalart-Allmaras (1992) 1-equation model, principally designed for computing attached flows on airfoils and the Kok model (Kok & Spekreijse, 2000; Brandsma et al., 2001) which is a linear 2-equation EVM that solves an equation for $\tau \propto k/\varepsilon$, in place of ε , wherein the production term employs the mean vorticity rather than strain rate if that leads to larger values of τ (and thus lower values of ε). The model's novelties had been explicitly calibrated for detached vortices.

Wall boundary conditions have been applied by way of analytic wall functions (Craft et al., 2002) to avoid the excessively fine mesh needed to resolve the viscous sublayer itself. While these have been widely validated in non-equilibrium wall flows, they do not permit the correct resolution of strong velocity skewing across the sublayer. However, comparative tests of the $k-\varepsilon$ model with wall functions and with a model providing a 'low-Reynolds-number' treatment across the sublayer (the 1-equation scheme of Wolfshtein, 1969) showed very little effect of this refined modelling. Such sublayer modelling was therefore not extended to other models and runs.

Numerical Resolution

The flow over the wing and near-field development of the vortex have been computed with STREAM (Lien & Leschziner, 1994). This is a fully 3D, elliptic finite-volume solver based on general curvilinear coordinates using the Rhie & Chow (1983) smoothing algorithm and employing the SIMPLE pressure-correction scheme. Convection is handled via a 2nd-order TVD scheme, initially on all variables but, as tests showed negligible effects, thereafter on just mean-flow variables (with turbulence variables, whose level is dominated by source-terms rather than convection, discretized via upwind differencing). The block-structured grid was created with the commercial meshing code ICEM. Because of the relatively large wing relative to the wind-tunnel dimensions, the whole wind-tunnel was included in the grid, the upstream boundary being placed at $x/c = -1.738$ where it was established the wing had no effect on the flow. (The streamwise coordinate, x , has its origin at the trailing edge of the airfoil.) The downstream boundary was placed at $x/c = +0.678$. For the computations reported here 4.2 million cells in 26 blocks were adopted, corresponding to a maximum grid spacing of $5 \times 10^{-3}c$ as recommended in Dacles-Mariani et al. (1995) while, for cells adjacent to the airfoil, the height normal to the surface was around $1 \times 10^{-3}c$ which typically gave values of y^+ at the near-wall node in the range 40-100. A sample of the grid on the wing surface and wing-root wall is shown in Fig. 1.

The block structured grid caused grid refinements around the airfoil to be propagated downstream to regions where refinement was not needed while leaving the vortex itself under-resolved. The final computations were thus performed in two stages. The first stage used the grid as described while the second limited attention to the wake region, adopting a purely Cartesian mesh of 4.3 million cells clustered around the vortex with an upstream boundary just downstream of the wing ($x/c = +0.001$). The conditions applied at this boundary were those interpolated from the best of the first-stage computations.

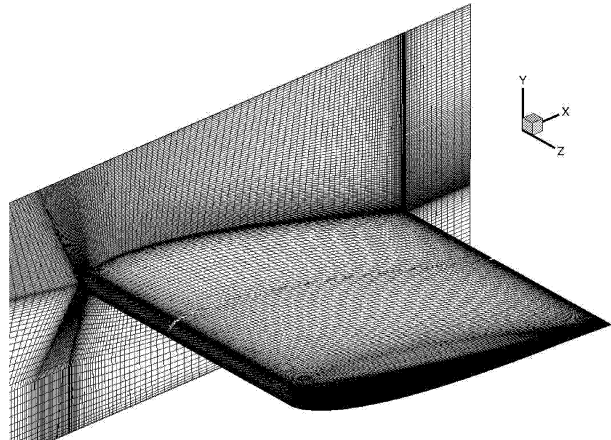


Figure 1: Wing and wing-root wall surface grids.

CONSIDERATION OF THE RESULTS

To give an overall impression, Fig. 2 shows the streamlines near the wingtip and pressure contours computed with the TCL model. This shows clearly the shed streamwise vortex and the associated low pressure at the vortex core. To provide a quantitative comparison, Fig. 3 shows the variation downstream of the axial velocity at the centre of the vortex. The experimental data show this to reach a maximum some 77% greater than the approach velocity, U_∞ , just before the end of the wing and thereafter there is a very slow decay. All the computational models except that of Spalart & Allmaras show reasonable agreement with the data over the wing itself, underlining the fact that the vortex creation is driven by inviscid effects associated with the pressure difference on the pressure and suction surfaces of the wing. The poor behaviour with the Spalart-Allmaras model serves to underline that it is a simple model that has been very carefully tuned for attached boundary layers and should not be expected to provide useful predictions beyond that regime.

Downstream of the wing there is a wide variation of behaviour exhibited across the models. This is because the decay of axial velocity is strongly linked to the decay of the vortex: as the angular momentum is dispersed by turbulent diffusion the pressure at the vortex centre rises causing the axial velocity to decay. The linear $k-\varepsilon$ EVM is insensitive to the stabilization brought about by the vortex and predicts a very rapid decay of the axial velocity. What surprised us was that the non-linear EVM performed nearly as poorly despite its earlier satisfactory handling of swirling flow in a pipe (Craft et al., 1996). Other studies of swirling free wakes (Robinson, 2001; Suga et al., 2000) have also shown indifferent agreement of a wake-

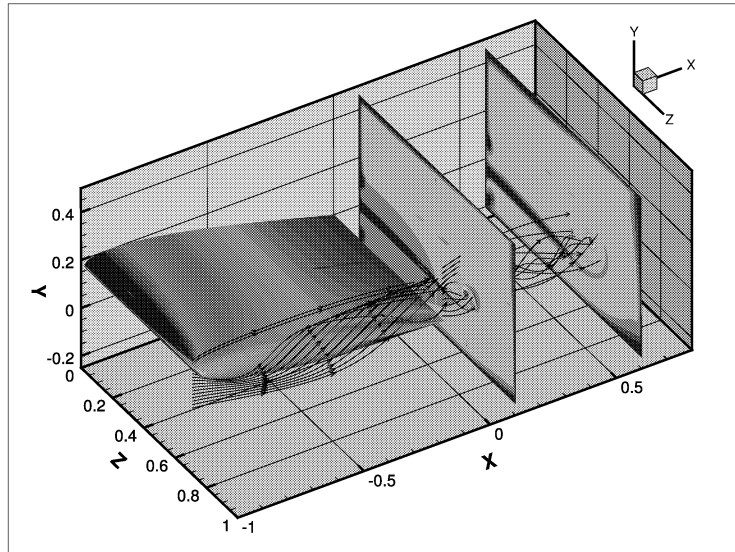


Figure 2: Computed streamlines and pressure contours using the TCL model.

vortex using (effectively) this NLEVM. Clearly further work is needed on optimizing the model's coefficients. The Kok model gives a significantly slower decay of velocity but it needs to be noted that it is a model that has been developed to handle precisely the type of flow here considered. The closest agreement was achieved by the TCL second-moment closure whose empirical coefficients have been chosen by reference to flows in simple shear. Nevertheless, that model too displayed an appreciably faster decay of wake-centre velocity than the data.

The *numerical* accuracy of the downstream vortex then came into question. The grid refinements designed to resolve in fine detail the boundary layers on the wing gave a far from optimum distribution in the wake. As noted above, a separate set of computations was therefore made, starting just downstream of the airfoil and using the computed values from the full-field computations to provide the entry conditions. The results for the TCL model in this case mimicked very closely the reported experimental development (see Fig. 4). Accordingly, the flow downstream of the airfoil was re-computed for

all the other models on the same grid using, in all cases, the TCL results to provide inlet conditions for the calculations. Figure 4 shows the same relative behaviour for the models as previously but the comparison now enables the shortcomings in predicting the vortex decay to be separated from other model weaknesses.

A more complete picture of the vortex-jet/wake development for all the models except the Spalart-Allmaras is shown in the cross-sectional views of Figs. 5–8. The axial velocity at the final station, shown in Fig. 5, presents striking differences among the models. For the linear EVM, the jet associated with the vortex has changed to a wake while the non-linear EVM exhibits a velocity peak within the vortex core but a wake beyond. The Kok model predictions do still show a velocity peak, but its magnitude is much smaller than the experimental measurements. In contrast the TCL scheme exhibits a pattern that closely mimics the data. A similar range of behaviour is found also in the magnitude of the cross-sectional plane velocity $(V^2 + W^2)^{1/2}$ shown in Fig. 6. While

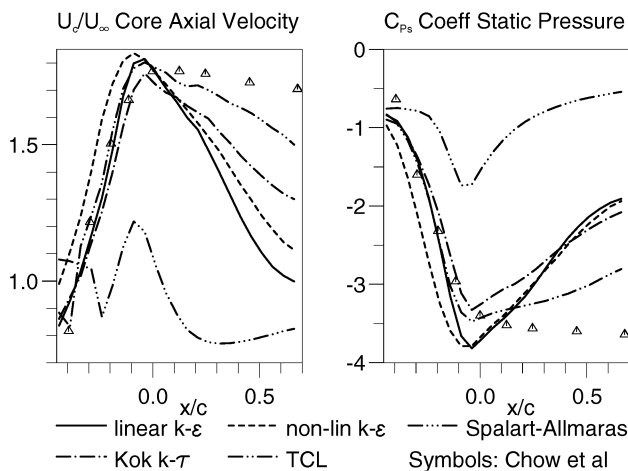


Figure 3: Downstream variation of axial velocity at the vortex centre.

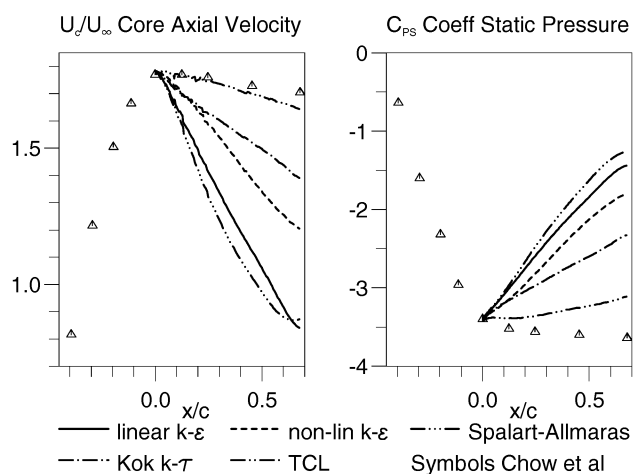


Figure 4: Vortex centre axial velocity development using the refined downstream grid.

the linear EVM predicts a too rapid dispersal at all radii from the vortex centre, the non-linear model shows a much reduced dispersal rate in the inner core where the angular momentum of the vortex is increasing with radius but appears to have caused a faster rate of radial diffusion beyond that core. The Kok model shows some improvement, but it is again the TCL model that most closely mimics the measured distribution of velocity.

The turbulence velocities likewise show striking differences, exemplified in Fig. 7 by the contours of $\overline{u^2}/U_\infty^2$. The linear and non-linear EVM display high residual levels of turbulence, with the non-linear model (and the Kok model) having a striking “hole” in the region of the vortex centre. The experimental data, in contrast, show turbulence to be confined to a small zone coinciding closely with the region where the angular momentum is increasing. This feature of the experiments is puzzling for, once the flow has had sufficient time to develop, this inner viscous core would be expected to be laminar. Thus, it may well be the case that the “turbulence” shown in the experiments is a spurious indicator caused by precessing of the vortex. Such behaviour has been reported in other swirling flows in the literature, for example Morse (1980). Certainly the TCL predictions show no sign of a peak in turbulence within the vortex core; indeed, at no point do the normalized turbulent stresses exceed a level of 0.002 (i.e. a turbulence intensity of some 4.5%).

Finally, the shear stress \overline{uv} contours in Fig. 8 also highlight the failure of the linear and non-linear EVM’s, both of which return far too high shear stress magnitudes. The TCL and Kok models return much lower levels, generally closer to those in the measurements. The higher measured levels towards the vortex centre may again be due to precessing of the vortex, as explained above.

CONCLUSIONS

This study of the performance of five turbulence models in reproducing the near-field behaviour of the wing-tip vortex measured by Chow et al. (1997) has shown that:

- Linear eddy viscosity models lead to a much too fast dispersal rate and should not be used for such flows.
- While the non-linear EVM of Craft et al. (1996) leads to a diminution of mixing in the vortex core, its overall performance is scarcely better than the linear EVM. Further re-tuning of some of the empirical coefficients needs to be undertaken, perhaps by making them functions of the dimensionless vorticity:strain ratio.
- The Kok model, which has been designed for computing detached vortices, performed better than the linear and non-linear EVM’s, but still produced too rapid a dispersal of the accelerated vortex core.
- The TCL second-moment closure which, over the past decade, has been applied by the UMIST team to a wide range of complex flows near walls, returns, in most respects, close agreement with experiment in this complex free shear flow.
- The most striking area of disagreement between experiment and the TCL computations is in the level of turbulence near the vortex centre. It is suggested that the discrepancy may possibly be associated with a precessing of the vortex core in the experiment.

ACKNOWLEDGEMENTS

The work reported has been undertaken as part of the M-DAW programme, supported by the European Commission through research grant G4RD-CT-2002-00837. Overall direction of the programme has been provided by Mr Alan Mann (Airbus-UK) and Dr Eberhard Elsholz (Airbus-D). Computational resources provided by the University’s Mason Centre for Environmental Flows are acknowledged. Authors’ names appear alphabetically.

REFERENCES

- Brandsma, F.J., Kok, J.C., Dol, H.S. and Elsenaar A., 2001, “Leading edge vortex flow computations and comparison with DNW-HST wind tunnel data”, Tech Rep NLR-TP-2001-238, NLR.
- Chow, J., Zilliac, G. and Bradshaw, P., 1997, “Turbulence measurements in the near field of a wingtip vortex”, NASA Tech Mem 110418, NASA.
- Craft, T.J., Launder, B.E. and Suga, K., 1996, “Development and application of a cubic eddy-viscosity model of turbulence”, *Int. J. Heat Fluid Flow*, Vol. 17, pp. 108-115.
- Craft, T.J. and Launder, B.E., 2001, “Principles and performance of TCL-based second-moment closures”, *Flow, Turbulence and Combustion*, Vol. 66, pp. 355-372.
- Craft, T.J., Gerasimov, A.V., Iacovides, H. and Launder, B.E., 2002, “Progress in the generalization of wall-function treatments”, *Int. J. Heat Fluid Flow*, Vol. 23, pp. 148-160.
- Dacles-Mariani, J., Zilliac, G., Chow, J.S. and Bradshaw, P., 1995, “Numerical/experimental study of a wingtip vortex in the near field”, *AIAA J.*, Vol. 33, pp. 1561-1568.
- Kok, J.C. and Spekreijse, S.P., 2000, “Efficient and accurate implementation of the $k-\omega$ turbulence model in the NLR multi-block Navier-Stokes system”, Technical Report NLR-TP-200-144, NLR.
- Launder, B.E. and Li, S-P., 1994, “On the elimination of wall-topography parameters from second-moment closure”, *Phys Fluids*, Vol. 6, pp. 999-1006.
- Lien, F-S. and Leschziner, M.A., 1994, “A general non-orthogonal finite-volume algorithm for turbulent flow at all speeds incorporating second-moment turbulence-transport closure”, *Comp. Meth. Appl. Mech. Eng’g*, Vol. 114, pp. 123-167.
- Morse, A.P., 1980, “Axisymmetric free shear flows with and without swirl”, PhD thesis, University of London.
- Rhie, C.M. and Chow, W. L., 1983, “Numerical study of the turbulent flow past an airfoil with trailing edge separation”, *AIAA J.*, Vol. 21, pp. 1525-1532.
- Robinson, C.M.E., 2001, “Advanced CFD modelling of road-vehicle aerodynamics”, PhD Thesis, UMIST.
- Spalart, P. and Allmaras, S., 1992, “A one-equation turbulence model for aerodynamic flows”, AIAA Paper 92-0439, Reno, Nevada.
- Suga, K., Nagoaka, M., Hommuchi, N., Abe, K., Kondo, Y., 2000, “Application of 3-eq cubic EVM to 3D turbulent flows by unstructured grid method”, *Proc 3rd Int. Symp. on Turbulence, Heat & Mass Transfer* (eds. Nagano, Hanjalic & Tsuji), Aichi Shuppan.
- Wolfshtein, M., 1969, “The velocity and temperature distribution in one-dimensional flow with turbulence augmentation and pressure gradient”, *Int. J. Heat Mass Transfer*, Vol. 12, pp. 301-318.

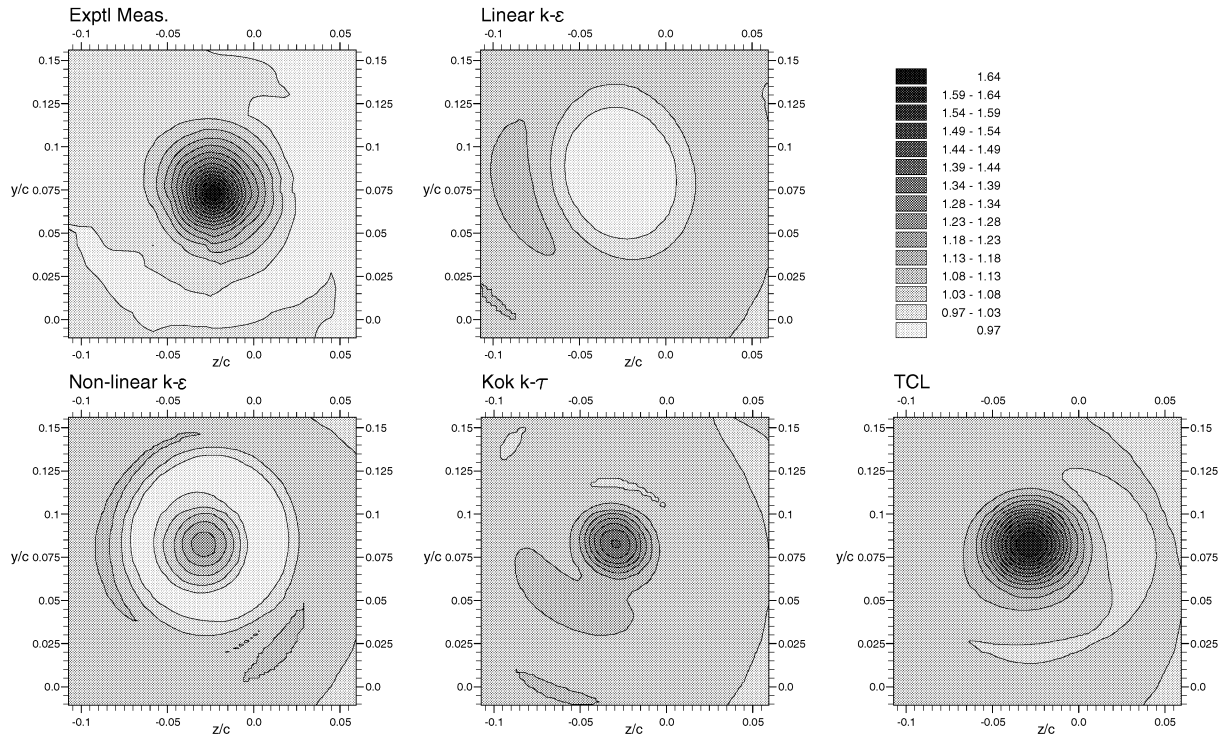


Figure 5: Contours of axial velocity, U/U_∞ , at $x/c = 0.678$.

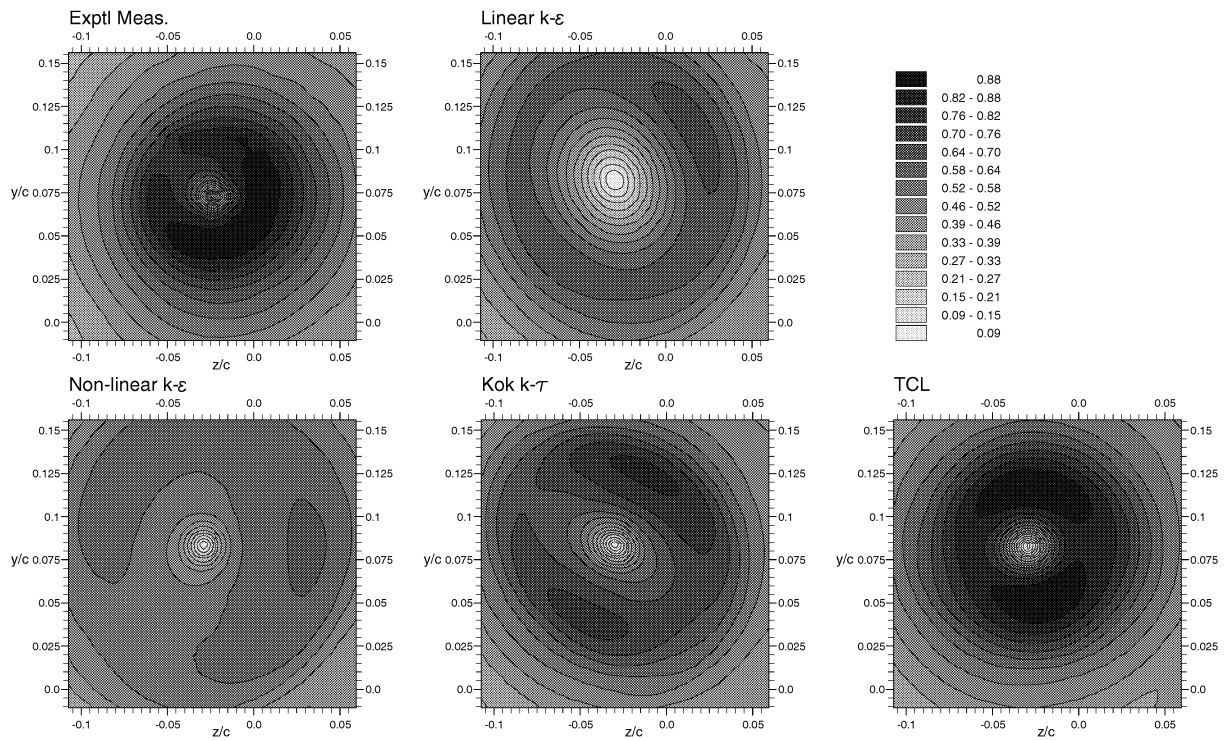


Figure 6: Contours of cross-flow velocity, $(V^2 + W^2)^{1/2}$, at $x/c = 0.678$.

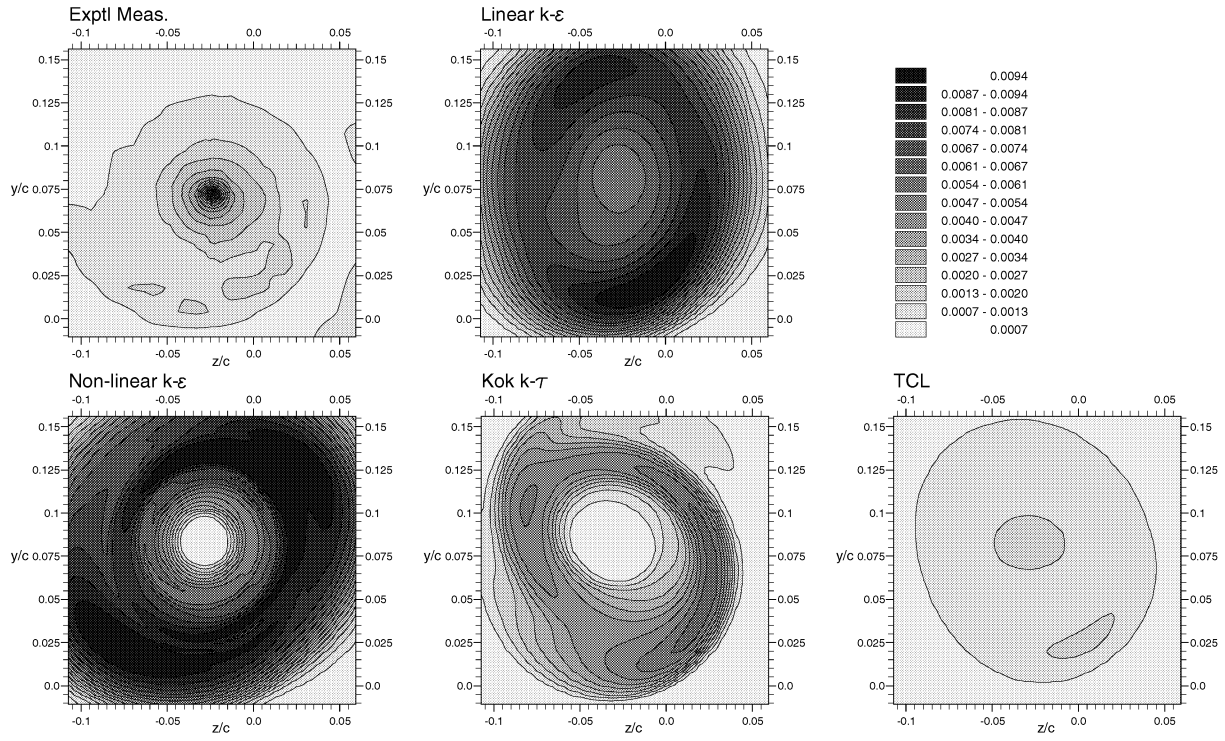


Figure 7: Contours of axial normal stress, $\overline{u^2}/U_\infty^2$, at $x/c = 0.678$.

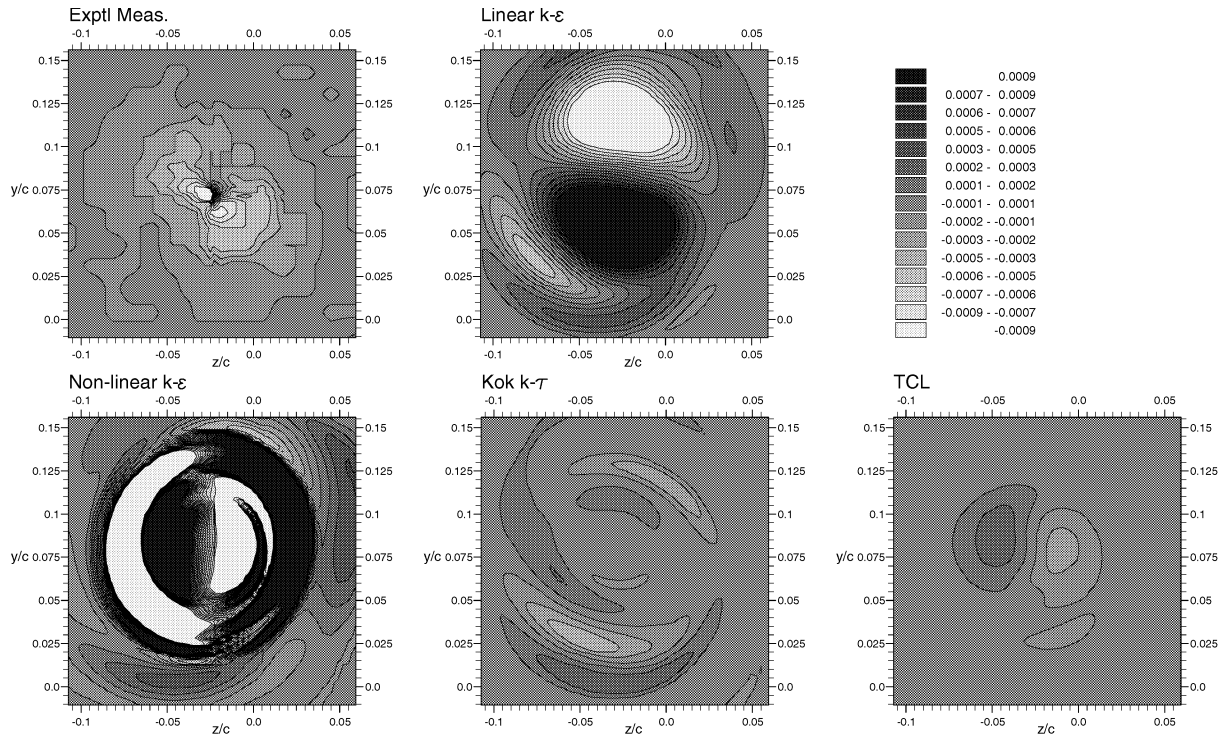


Figure 8: Contours of the turbulent shear stress \overline{w}/U_∞^2 , at $x/c = 0.678$.